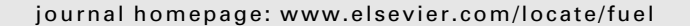


Contents lists available at ScienceDirect

Fuel





Characterization of coal ash released in the TVA Kingston spill to facilitate detection of ash in river systems using magnetic methods



Ellen A. Cowan a,*, Daniel P. Gaspari a,1, Stefanie A. Brachfeld b, Keith C. Seramur a

HIGHLIGHTS

- Kingston coal ash increases magnetic susceptibility of riverbed sediment.
- Fluvial transport both enriches and dilutes the magnetic fraction of coal ash.
- Micron-size magnetite and maghemite occur within aluminosilicate spheres.
- Magnetospheres dominate the magnetic signal in the Watts Bar watershed.

ARTICLE INFO

Article history: Received 31 March 2015 Received in revised form 24 June 2015 Accepted 25 June 2015 Available online 2 July 2015

Keywords: Magnetospheres Magnetic susceptibility SEM-EDS Kingston ash spill Environmental monitoring

ABSTRACT

The magnetic properties of riverbed samples collected after the 2008 Tennessee Valley Authority (TVA) coal ash spill in Kingston, Tennessee are investigated. Coal ash persists in this fluvial environment because 400,000 m³ of ash remains in areas that were not dredged. The magnetic fraction is low in comparison to other coal ash; 1.4 wt% in a sample from the failed ash storage cell increasing to 3.0 wt% in riverbed samples in the Emory River near the spill. Thermomagnetic analysis, XRD, SEM and polarized light microscopy identified magnetospheres with magnetite and maghemite from the Kingston coal ash as the magnetic carrier. Anthropogenic nonspherical magnetic particles are introduced from the industrialized Tennessee River watershed prior to reaching the Watts Bar Reservoir. A bivariate plot of anhysteretic remanent magnetization (ARM) versus mass-normalized low field magnetic susceptibility (χ_{LF}) models the mixing of ash in the rivers, identifying both enrichment of magnetospheres by sorting near the spill and dilution with native sediment downstream. Concentration-dependent magnetic parameters in ash-bearing samples are approximately 2–56 times stronger than those of the ash-free watershed samples. This study supports the use of magnetic parameters to track the ash as it is eroded and transported 71 km downstream to the Watts Bar Dam and suggests that χ_{LF} can be utilized to track the migration of coal ash in other river systems.

© 2015 Elsevier Ltd. All rights reserved.

1. Introduction

For over 50 years, coal-burning electrical utilities have generated billions of tons of coal combustion byproducts (CCBs), mainly coal ash, much of which has been conveniently stored next to waterways across the United States in unlined ponds or lagoons [1]. This practice received little attention from the public until December 2008, when 4.1 million m³ of coal ash at the

Tennessee Valley Authority (TVA) Kingston Fossil Plant in Kingston, Tennessee spilled into the Emory River in the upper reaches of the Watts Bar Reservoir system [2]. Due to its association with heavy metals, coal ash is now recognized by the public as a substantial threat to drinking water, recreation, aquatic organisms and habitat [3,4]. Most of the coal ash spilled at Kingston was mechanically and hydraulically dredged, however 400,000 m³ was mixed with legacy contaminants, primarily ¹³⁷Cs and Hg released from US Department of Energy facilities at Oak Ridge [2] and another 92,000 m³ eroded during a flood prior to dredging [5]. The remaining ash has been and continues to be scoured, suspended and mixed with riverbed sediments as it is transported 71 km downstream to the Watts Bar Dam where it will be buried within reservoir sediment. TVA conducted a Baseline Ecological

^a Department of Geology, Appalachian State University, Box 32067, Boone, NC 28608, USA

^b Department of Earth and Environmental Studies, Montclair State University, Montclair, NJ 07043, USA

^{*} Corresponding author. Tel.: +1 828 262 2260; fax: +1 828 262 6503.

E-mail addresses: cowanea@appstate.edu (E.A. Cowan), gaspari@g.clemson.edu (D.P. Gaspari), brachfelds@mail.montclair.edu (S.A. Brachfeld), seramurkc@appstate.edu (K.C. Seramur).

¹ Current address: Department of Environmental Engineering and Earth Science, Clemson University, Clemson, SC 29634, USA.

Risk Assessment to evaluate the potential effects of this residual ash on biota and concluded that benthic invertebrates and insectivorous birds have the potential to be adversely affected [6]. The Engineering Evaluation/Cost Analysis (EE/CA) performed by TVA was the basis for selecting Monitored Natural Recovery (MNR) for remediation of the residual ash with verification by long-term sampling [6,7]. Once coal ash is diluted with natural sediment and incorporated into the riverbed, the concentration of ash cannot be visually quantified. Therefore, the distribution of ash in riverbed sediments is currently monitored by point counting aliquots of sediment under polarized light microscopy (PLM), while the distribution of hazardous trace metals, particularly arsenic and selenium is determined by chemical analysis [7].

We have demonstrated that a time efficient and cost effective method of distinguishing ash from background watershed sediment could be developed by measuring the mass-normalized low field magnetic susceptibility (χ_{LF}) of riverbed sediment [8]. Within the area affected by the spill, we determined that γ_{IF} is positively correlated with the measured percent total ash determined with PLM in the Watts Bar Reservoir system [8]. Samples with $\chi_{LF} \leq 1.0 \times 10^{-7} \,\mathrm{m}^3/\mathrm{kg}$ were devoid of ash or had negligible ash content, and samples with $\chi_{LF} > 3.0 \times 10^{-6} \,\mathrm{m}^3/\mathrm{kg}$ were composed of greater than 15% ash. Samples with $\gamma_{LF} \ge 1.0 \times 10^{-5} \,\mathrm{m}^3/\mathrm{kg}$ were composed of >80% ash [8]. In the initial study, we identified that the magnetic component occurred within the spherical fraction of coal ash but we could not determine from statistical analysis of the bulk samples whether it was preferentially within the black, orange, or clear spheres. In this study, we collect a suite of analyses, including PLM, X-ray diffraction (XRD), scanning electron microscopy (SEM) and rock magnetic measurements to characterize the mineralogy, grain size and morphology of the magnetic carrier responsible for χ_{LF} measurements above background in the rivers affected by the Kingston spill. We also investigate the magnetic characteristics of samples from areas of the Tennessee River, that were not impacted by the Kingston spill and contribute sediment to the Watts Bar Reservoir (Fig. 1). Our immediate goals are to identify the magnetic carrier of the χ_{LF} signal, the morphology of the magnetic fraction, and domain state of the coal ash magnetospheres and the natural watershed sediment such that these two components can be distinguished and tracked. The long-term goal is to develop magnetic proxies of coal ash within river sediment to more easily and inexpensively assess its downstream transport after release into the aquatic environment. This approach has immediate and practical use because EE/CAs show that it is impractical and expensive to completely remove large volumes of fine-grained coal ash from waterways after a spill, thus requiring long-term monitoring of residual ash within the aquatic environment.

2. Materials and methods

Ash samples from the failed storage cell, 16 box core samples of ash/sediment mixtures from the riverbed, 2 composite sediment samples from upstream on the Emory and Clinch Rivers, and 8 samples from the Tennessee River both downstream and upstream of the spill were used in this study (Fig. 1; Table 1). Sample collection methods are described in [8]. Clinch Ref. and Emory Ref. are composites of samples collected upstream of the spill (CRM 7.5 and CRM 6.5 and ERM 10.0 and ERM 8.0 respectively) and represent the native watershed sediment.

2.1. Magnetic measurements

Magnetic measurements were made at the Department of Earth and Environmental Studies at Montclair State University. Air-dried

bulk sediment was packed into size 4 gelatin capsules and the mass was recorded. Mass-normalized low field magnetic susceptibility (γ_{LF}) was measured on an AGICO KLY-4 Kappabridge. Anhysteretic remanent magnetization (ARM) was imparted in a peak alternating field of 100 mT and a steady DC field of 0.05 mT and measured on an AGICO JR-6 spinner magnetometer. Hysteresis parameters including saturation magnetization, saturation remanence, coercivity, and coercivity of remanence, $(M_S, M_R,$ H_C , H_{CR} respectively) were measured on a Princeton Measurement Corp. 3900 04 Vibrating Sample Magnetometer (VSM) using a peak field of 1 T. Curie temperature analyses were conducted on bulk sediment samples using the AGICO KLY-4 Kappabridge with a CS-3 furnace attachment. All samples were measured in a flowing argon atmosphere during heating and cooling between room temperature and 700 °C. In addition, a second Ash 2-1 sample was measured in air.

2.2. Magnetic separation, PLM, XRD, and SEM

Separation and characterization of the magnetic fractions were conducted in the Department of Geology at Appalachian State University. Bulk samples were subsampled and mixed to form a sediment/water slurry in an approximate ratio of 1:3. The slurry was poured into a series of 150 ml beakers with 4 magnets attached to their base. After vigorous mixing, the slurry settled for 10 s before being decanted into the next beaker. Particles that remained attached to the bottom of the beaker were rinsed until only the magnetic particles remained. This process was repeated for four beakers and all the magnetic material from the sample was combined into a magnetic fraction (MF) sample.

Smear slides were made by spreading a small amount of MF across the surface of a microscope slide with a toothpick. The slide was fixed using Loctite Gel Control Superglue. Five hundred points were counted at 200× magnification using a Zeiss Point Counter mounted on a petrographic microscope [8]. Following our previous PLM methods we identified particles as spherical or non-spherical. Spherical particles were further classified by color; either black, orange or clear (Table 1).

XRD patterns of powdered coal ash and magnetically separated ash from the storage cell (Ash 2–1) were obtained using a Shimadzu XRD-6000 diffractometer with Cu K α radiation (tube voltage 40 kV and 30 mA tube current) by scanning from 2 to 70° (2 θ) at a speed of 2°/min.

Morphology of the MF of samples in Table 1 was imaged on a Quanta FEI 200 Scanning Electron Microscope (SEM) in high vacuum mode at 20 kV. Samples were mounted on aluminum stubs and coated with gold. Backscattered electron imaging (BSE) and Energy Dispersive Spectrometry (EDS) were used to identify morphology and qualitative composition of samples.

3. Results

3.1. Magnetic mineralogy

Thermomagnetic curves from the storage cell ash sample (Ash 2–1) measured in argon exhibit a rapid decay of χ_{LF} between 500 and 600 °C. The heating and cooling curves are reversible over this temperature range (Fig. 2A). Curie temperatures estimated using the "two tangents" method [9] fall between 580 and 600 °C, indicating that the magnetic carriers are magnetite and slightly oxidized magnetite (Fig. 2A–F)[10]. The cooling curve is slightly higher than the heating curve below 500 °C. Riverbed samples (all measured in argon) with MF > 1% display thermomagnetic curves that resemble the pure ash sample (Fig. 2D).

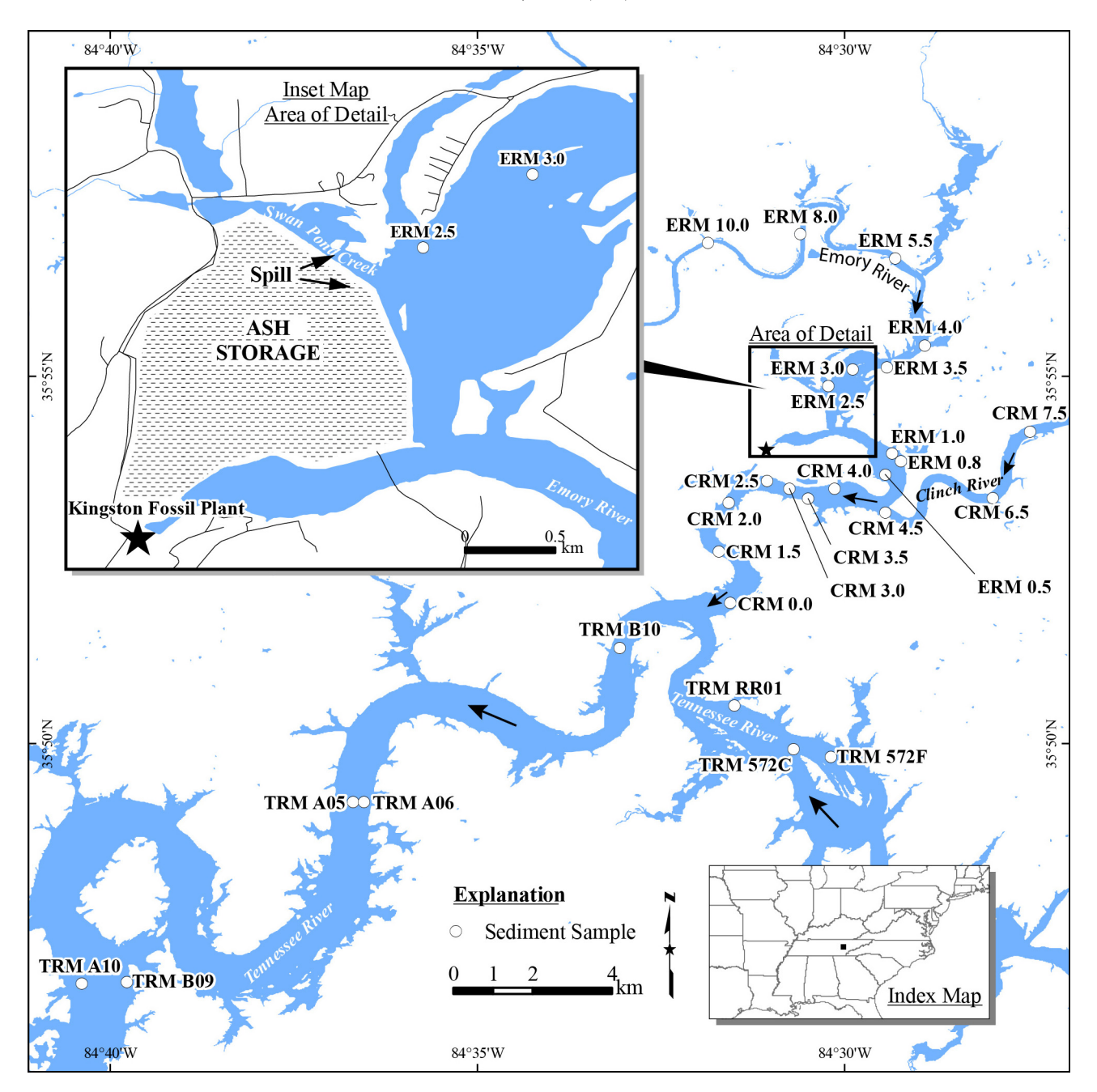


Fig. 1. Location map showing sample collection sites within the upper Watts Bar Reservoir system. Inset map shows the location of the coal ash spill from the storage cell at the TVA Kingston Fossil Plant into the Emory River.

A fresh sample of Ash 2–1 was also measured in air. Ash 2–1 shows little difference between the air and argon thermomagnetic curves below 600 °C (Fig. 2A and B). In argon, the heating and cooling curves are flat between approximately 600 and 700 °C. During heating in air, χ_{LF} shows a continued steady decay between 600 and 700 °C, and the heating and cooling curves are reversible in this temperature range (Fig. 2C). This suggests that maghemite in the sample converts to hematite when heated in air, and the newly formed hematite is responsible for the susceptibility signal above 600 °C (Fig. 2C).

Riverbed samples that lack coal ash from the Kingston spill (ERM and CRM Reference (not shown) and TRM 572-C) have strongly irreversible heating and cooling curves, with the cooling curve much stronger than the heating curve (Fig. 2E and F).

These samples display a broad alteration peak between 450 and 540 °C. In addition, they display an interval of increasing χ_{LF} between 260 and 300 °C, followed by decreasing χ_{LF} to 400 °C. The initial increase in χ_{LF} and the subsequent alteration could be due to conversion of iron rich clays to magnetite [11]. Alternately, the feature at 260–300 °C could represent the lambda transition in antiferromagnetic hexagonal pyrrhotite (Fe₉S₁₀) [12]. No iron sulfides were observed in the MF, although it is possible they were not recovered in the extraction process. The decrease in signal between 300 and 400 °C could be due to maghemite within the natural watershed sediment. This comparison of ash-bearing and ash-free riverbed samples confirms that the χ_{LF} signal originates primarily from the magnetite introduced into the watershed by Kingston ash.

 Table 1

 Magnetic and morphological characteristics of the magnetic extract of samples from the storage cell, Emory and Clinch Rivers and the Tennessee River (TN R.), upstream and downstream of the Kingston spill.

Location	Sample number	^a MF (%)	$^{b}X_{LF}$ (m 3 /kg)	^c ARM (Am²/kg)	^d Black spheres (%)	Orange spheres (%)	Clear spheres (%)	Nonspherical particles (%)
Ash Storage	ASH 2-1	1.40	5.14×10^{-6}	3.78×10^{-4}	84.4	2.0	1.8	11.2
Emory River	ERM 2.5	2.68	9.42×10^{-6}	5.78×10^{-4}	92.2	1.0	2.4	4.2
Emory River	ERM 0.5	2.97	8.46×10^{-6}	5.24×10^{-4}	89.8	1.6	1.4	6.8
Clinch River	CRM 3.5	1.89	5.87×10^{-6}	4.88×10^{-4}	90.8	1.6	2.6	4.8
Clinch River	CRM 2.5	1.33	4.64×10^{-6}	4.14×10^{-4}	90.0	1.4	2.2	5.8
Clinch River	CRM 1.5	0.55	2.28×10^{-6}	3.06×10^{-4}	90.8	1.2	1.4	5.8
Clinch River	CRM 0.0	1.92	6.28×10^{-6}	5.12×10^{-4}	90.4	2.0	1.6	5.2
Downstream TN R.	TRM B10	0.73	3.05×10^{-6}	4.00×10^{-4}	91.0	0.8	1.2	7.0
Downstream TN R.	TRM A06	0.32	1.80×10^{-6}	3.85×10^{-4}	87.4	1.8	1.8	9.0
Downstream TN R.	TRM A05	0.07	6.73×10^{-7}	2.51×10^{-4}	77.6	1.0	1.8	19.0
Downstream TN R.	TRM B09	1.57	5.39×10^{-6}	4.88×10^{-4}	91.6	0.8	1.6	6.0
Downstream TN R.	TRM A10	0.02	4.99×10^{-7}	2.12×10^{-4}	79.6	1.6	1.6	17.0
Upstream TN R.	TRM RR01	0.03	7.28×10^{-7}	2.17×10^{-4}	19.6	1.0	0.4	78.4
Upstream TN R.	TRM572-F	0.02	7.33×10^{-7}	2.58×10^{-4}	8.8	0	0.2	90.6
Upstream TN R.	TRM 572-C	0.03	5.01×10^{-7}	1.34×10^{-4}	9.6	0.2	1.4	88.6

^a MF = Magnetic fraction separated from the bulk sample.

d Measured by point counting using PLM.

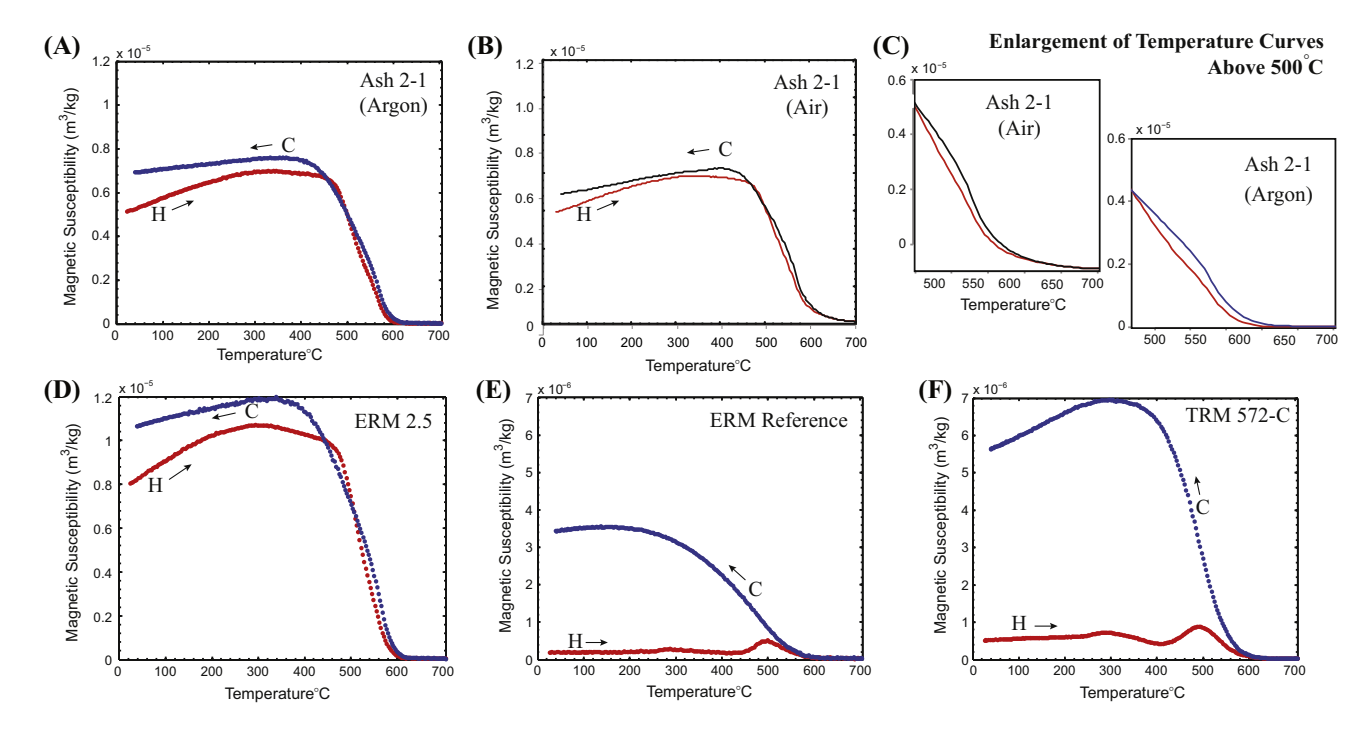


Fig. 2. Heating (red) and cooling (blue) curves for Ash 2–1 from the failed storage cell in an argon atmosphere (A), and in air (B), and enlargement of thermomagnetic curves above 500 °C from graphs A and B (C), riverbed sample containing coal ash at site ERM 2.5 (D). Samples upstream of the spill are shown for comparison (E, F). Note the change of scale on the vertical axis between A–D and E–F. (For interpretation of the references to colour in this figure legend, the reader is referred to the web version of this article.)

3.2. Magnetic grain size

The "Day Plot" [13] uses the hysteresis parameters $H_{\rm CR}/H_{\rm C}$ versus $M_{\rm R}/M_{\rm S}$ to estimate magnetic domain state populations within a sample set. The stable single domain (SSD, <0.05 μ m), pseudo-single domain (PSD, 1–10 μ m), and multidomain (MD, >10 μ m) field boundaries are calibrated only for magnetite and titanomagnetite [13]. Natural sediment contains a mixture of magnetic minerals and a range of grain sizes. Therefore, we use the Day Plot solely to visualize differences in magnetic mineral assemblages in ash-bearing and ash-free samples, and not for quantitative magnetic grain size determinations. All samples containing Kingston ash plot within a narrow cluster in the PSD field of the

Day Plot (Fig. 3). Samples from the Tennessee River watershed also plot within this cluster. In contrast, the reference samples plot far to the right or below this cluster. The Clinch reference sample has a higher $H_{\rm CR}/H_{\rm C}$ ratio than the ash-bearing samples. This could be due to the elevation of $H_{\rm CR}$ by minerals with high magnetocrystalline anisotropy, for example hematite and goethite [12]. The Emory reference sample has a low $M_{\rm R}/M_{\rm S}$ ratio relative to the ash-bearing samples.

3.3. Magnetic concentration

Anhysteretic remanent magnetization (ARM) is a laboratory-induced parameter in which the SSD and PSD grains

b,c Measured on bulk samples including the nonmagnetic fraction.

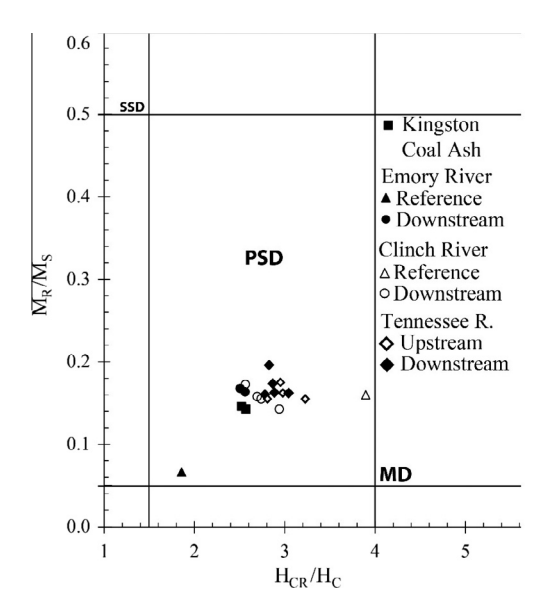


Fig. 3. Day Plot [13] indicating that all samples containing Kingston ash plot in a tight cluster within the pseudo-single domain (PSD) field. Ash-bearing samples from the Tennessee River watershed also plot within this cluster. Upstream ash-free reference samples from the Emory and Clinch Rivers plot outside this cluster. SSD = stable single domain, MD = multidomain.

are preferentially magnetized, contributions from multidomain grains are minimized, and contributions from superparamagnetic, paramagnetic, and diamagnetic grains are excluded. This contrasts with χ_{LF} , which represents the combined response of all components within a sample. A "Banerjee Plot" of ARM versus χ_{LF} (Fig. 4) can be used to discriminate different magnetic mineral populations [14]. The Emory-Clinch-Tennessee River sample set contains two distinct populations. The first population is defined by the linear array of points nearest the origin and is comprised of Emory and Clinch reference samples, and samples from the Tennessee River upstream of the confluence of the Clinch River $(R^2 = 0.87)$. The second population is defined by the linear array of fluvial samples with ARM > 1.5×10^{-4} Am²/kg ($R^2 = 0.88$). In each population, points that plot closer to the origin have a lower concentration of magnetic material [14,15]. The pure ash sample from the storage cell plots in the center of this array.

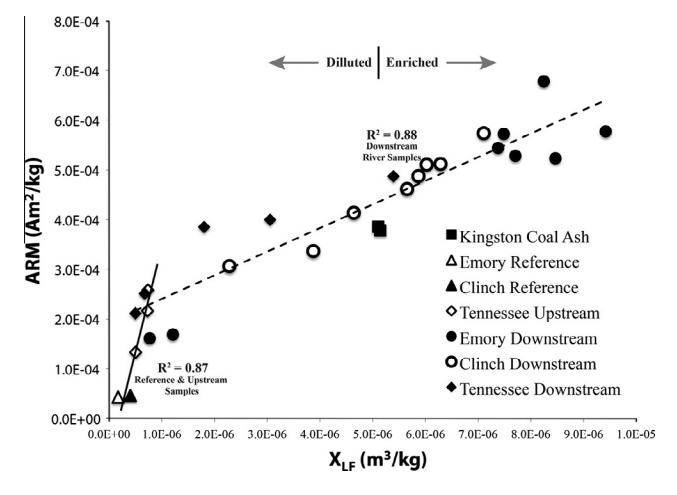


Fig. 4. Banerjee plot of ARM versus χ_{LF} for all samples analyzed in river system and the failed coal ash cell. Steeper (shallower) slopes indicating finer (coarser) grains. Distance from the origin along a given trend line is a function of the magnetic mineral abundance [14].

Concentration variations are caused by enrichment or dilution of the magnetic fraction of the ash in the river system. Enrichment of the MF occurs immediately adjacent to the spill. As magnetospheres are transported downstream they are diluted by watershed sediment (Fig. 4).

3.4. Magnetosphere abundance and morphology

The weight% MF in the sample collected from the failed storage cell was 1.4%. Once ash entered the Emory River, wt% MF increased to $\sim\!3.0\%<1$ km upstream from the spill location, and then decreased downstream to between 1.9% and 0.55% in the Clinch River (Fig. 1). Although CRM 0.0 is further from the spill, the % MF jumped from 0.55 to 1.92 (Table 1) at this station. This results from increased ash deposition at the confluence of the Tennessee River near this site. The wt% MF in samples from the Tennessee River upstream of the Clinch River ranged from 0.02% to 0.03% while those within the Tennessee River downstream of the Clinch River ranged from 0.02% to 1.6% (Table 1).

PLM showed morphological variability between the MFs extracted from sediments containing Kingston coal ash and the MFs of the upstream Tennessee River samples (Table 1). Black magnetospheres are the most common morphology in the MFs within riverbed samples downstream of the Kingston spill. The upstream Tennessee River samples are dominated by nonspherical black particles. The MFs of samples from the Tennessee River downstream of the Kingston spill consist predominantly of magnetospheres with nonspherical ash present in varying abundance (Table 1).

3.5. Mineralogy and morphology: XRD and SEM

XRD pattern of bulk ash from the storage cell indicates the presence of quartz, mullite and calcite but no peaks indicative of magnetic minerals are visible above the background (Fig. 5A). The diffraction pattern from the MF sample shows peaks of maghemite (cation-deficient magnetite), magnetite and small peaks of hematite and quartz (Fig. 5B) thus confirming the thermomagnetic analysis. The abundance of maghemite in this diffraction pattern may result from preferential analysis of the surface of the ash spheres,

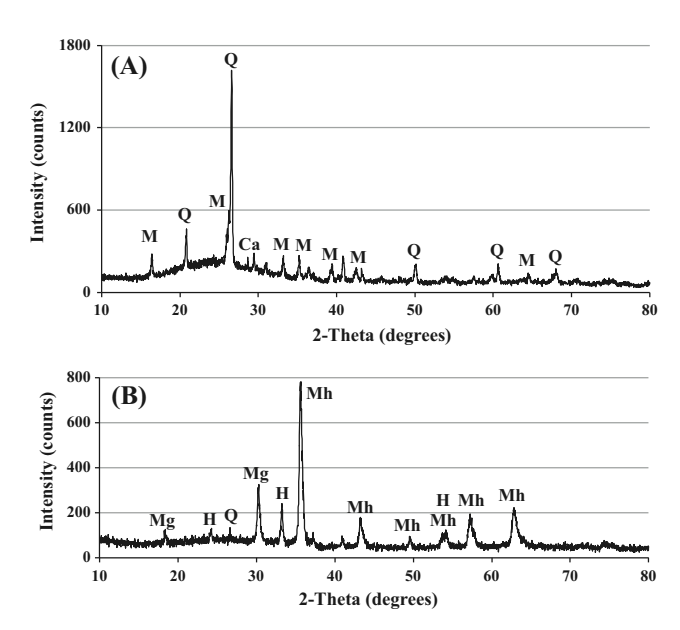


Fig. 5. X-ray diffraction (XRD) patterns of bulk coal ash (ASH 2-1) from the storage cell (A) and the MF of the same sample (B). M-mullite, Q-quartz, Ca-calcite, Mg-magnetite, Mh-maghemite, H-hematite.

which have undergone oxidation in the ash pond for some time. The spherical shape of the small ash particles likely resulted in rolling rather than crushing during XRD sample preparation.

SEM photomicrographs of the MF in samples collected downstream of the spill confirm the abundance of magnetospheres observed as black spheres with PLM (Fig. 6, Table 1). Magnetospheres average 10 μm in diameter [8] but range from a few microns to 50 µm. BSE images show different types of bright surface textures on dark spheres (Fig. 6) similar to samples collected directly from boilers or electrostatic precipitators and analyzed with SEM in other studies [11,16-19]. Individual crystals of ferrites are much smaller than the diameter of the sphere in which they reside. The broken exterior of a hollow ferrosphere shows larger well-formed crystals \sim 10 μ m in diameter (Fig. 7). These crystals occur throughout the interior of the sphere and within the glassy matrix of the shell. The Fe and O peaks in EDS spectra and triangular octahedral crystal habit are consistent with magnetite. which is likely undergoing surface oxidation to form maghemite (Fig. 6). The Tennessee River upstream of the spill is dominated by nonspherical particles in the MF. An example of these particles is shown in Fig. 8. EDS confirms that the bright areas have high relative abundance of iron.

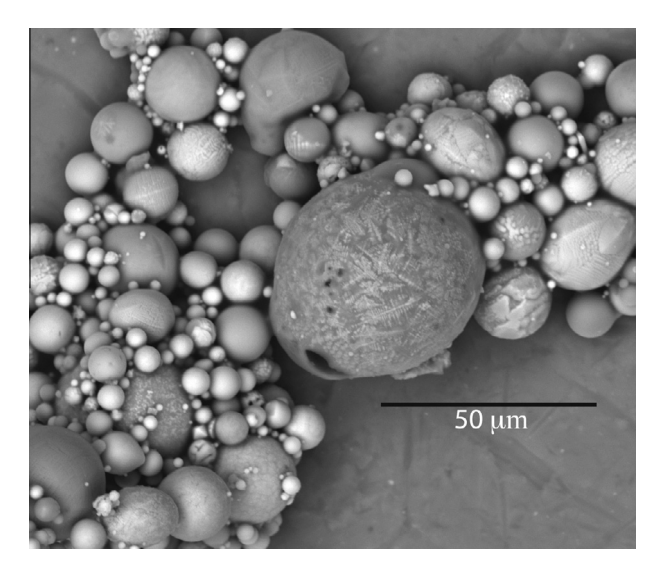


Fig. 6. Magnetospheres within the MF of sample CRM 0.0. Scale bar = $50 \mu m$.

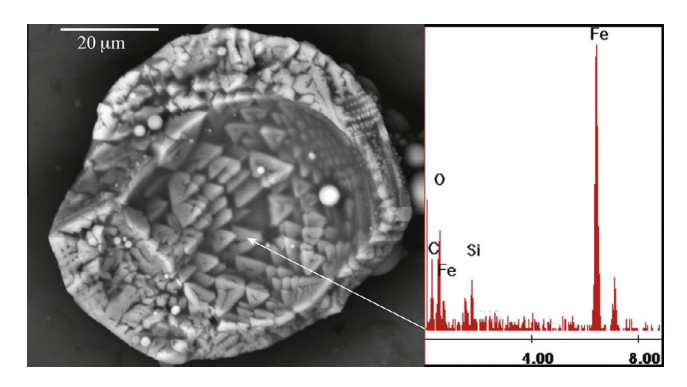


Fig. 7. SEM micrograph and EDS spectrum of a hollow ferrosphere from the failed ash cell displaying triangular octahedral crystals identified with EDS to contain Fe and O, consistent with magnetite. These crystals are less than 10 μ m in diameter, falling within the PSD size range for magnetite. Scale bar = 20 μ m.

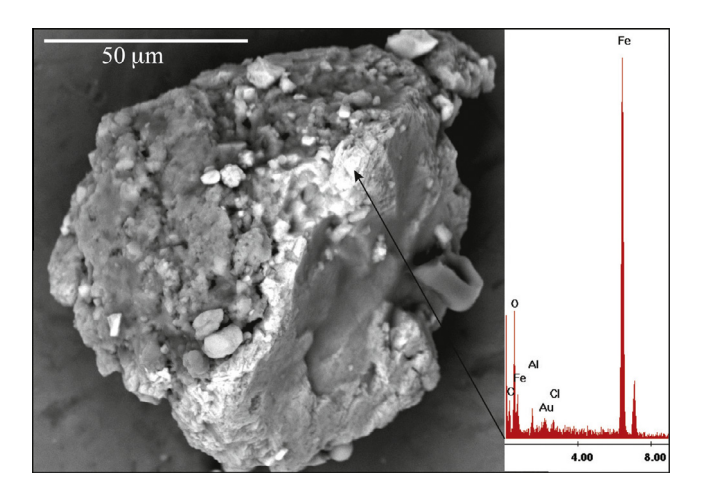


Fig. 8. Glassy nonspherical particle and EDS spectrum from the MF of upstream Tennessee River sample TRM RR01. The bright areas are iron rich. The edges of the grain are rounded suggesting river transport. Scale bar = $50 \mu m$.

4. Discussion

This study documents characteristic magnetic parameters that may be used to detect coal ash within riverbed sediment in a fluvial system. The magnetospheres in Kingston ash are similar in composition and magnetic properties to those produced as CCBs in other regions [20,21]. Although the wt% MF in samples from the storage cell is low (<2%), the amplitudes of χ_{LF} and ARM in Emory and Clinch River samples are, respectively, 2-56 times and 3-16 times greater than the watershed reference samples, allowing detection of Kingston ash mixed with watershed sediment. Other studies of samples collected from electrostatic precipitators report a range from 2 to 16 wt% MF within bulk coal ash samples [17,22]. Reworking by the Emory River increased the wt% MF to \sim 3% over 2.7 km of transport (Fig. 1). Likewise, the percent black spheres increased from 84% in the MF of stored ash to 92% in the MF of ERM 2.5, adjacent to the failed cell in the Emory River. This suggests that the denser magnetospheres are sorted and concentrated in riverbed sediment while the non-magnetic, non-spherical Kingston ash is entrained and transported downstream. This process effectively sorts the ash during river transport. The diameter of ash spheres falls into the silt-size range (3.9–62.9 μm), which can be sorted by low velocity currents. For example, preferential deposition of higher-density magnetic coal ash particles has been reported from the Yangtze River [23]. Our results demonstrate that Kingston ash has been transported to at least 37 km downstream from the spill site (to TRM A10) as of November 2010.

The ARM versus χ_{LF} plot shows enrichment where samples from the Emory and Clinch Rivers show higher concentrations of magnetic minerals than pure ash samples from the storage cell (Fig. 4). Ash from the spill is diluted as it is mixed with natural watershed sediment and follows the trend line toward lower ARM and χ_{LF} values. This dilution trend would be expected to continue downstream if the source ash were completely removed from the channel. However, no dredging was performed downstream of the ash storage area (see inset map, Fig. 1), or in the Clinch or Tennessee Rivers downstream of the spill and 400,000 m³ of ash is estimated to remain in the river system [2]. There are pockets of ash up to 0.125 m thick within the riverbed in the area between ERM 4.0 and CRM 3.0 [7]. High flow events are expected to erode these concentrated ash deposits thus increasing the availability of ash for downstream transport. Such events could be temporally monitored via the evolution of the ARM and χ_{LF} intensities of surface sediment samples as magnetospheres are eroded and transported downstream.

Riverbed samples from the upstream Tennessee River do not contain ash from the 2008 Kingston spill (Fig. 1). The MF from this region is dominated by nonspherical anthropogenic particles that contain magnetite, presumably originating from the industrial activities within the watershed [11]. These upstream Tennessee River samples have a lower χ_{LF} and ARM than samples containing Kingston ash (Fig. 4). Therefore, the source of these particles must have a lower magnetite concentration than the Kingston ash, though it is still sufficient to raise χ_{LF} and ARM above the Emory and Clinch River reference samples. Characterization of the pure source material from the upstream Tennessee River watershed would allow the development of distinct magnetic fingerprints for the Tennessee River anthropogenic particles versus Kingston ash. These could then be utilized as end-members in sediment mixing models that trace these particles and their associated contaminants within the Watts Bar Reservoir system.

5. Conclusions

This study presents magnetic characteristics of Kingston coal ash and background watershed sediment from the Emory, Clinch, and Tennessee Rivers. Native sediments within the Emory and χ_{LF} < 1 imes 10⁻⁶ m³/kg watersheds exhibit Clinch ARM $< 2.5 \times 10^{-4}$ Am²/kg. In samples where magnetospheres are rare, thermomagnetic curves are strongly irreversible and contain alteration features consistent with the conversion of iron-rich clays to magnetite. Kingston coal ash can be identified from the presence black magnetospheres and the combination $\chi_{LF} > 2 \times 10^{-6} \text{ m}^3/\text{kg}$, ARM > $3 \times 10^{-4} \text{ Am}^2/\text{kg}$, relatively invariant hysteresis parameters that plot within the PSD region of a Day Plot, and reversible thermomagnetic curves with Curie temperatures between 580 and 600 °C. These parameters allow us to estimate the concentration of Kingston ash in all of the samples that we have collected downstream of the 2008 spill, as far as 37 km, as well as identifying areas of magnetosphere enrichment and dilution. Other sources of anthropogenic particles originate within the heavily industrialized Tennessee River watershed upstream of the confluence with the Clinch River. These particles contain magnetite but they are nonspherical and have $\chi_{LF} < 5.0-7.0 \ (\times 10^{-7}) \ m^3/kg$. A pure sample of anthropogenic particles in the upstream Tennessee River is needed to allow quantitative estimates of Kingston ash versus Tennessee River watershed contributions to χ_{LF} and ARM downstream of the Clinch-Tennessee confluence. However, the available data demonstrates that magnetic parameters may serve as qualitative indicators of Kingston coal ash and ash-borne contaminants in the Emory, Clinch, and Tennessee Rivers as the ash travels downstream 71 km to the Watts Bar Dam. Our previous work showed that χ_{LF} corresponded with the percent total ash in riverbed sediments [8]. The strong χ_{LF} signal of PSD magnetite along with maghemite that likely resulted from cation substitution during ash weathering is in sharp contrast to the background magnetic signal derived from sedimentary rocks in the watershed. Therefore, the distinctive magnetic characteristics of Kingston coal ash confirm that magnetic susceptibility is useful and a potentially lower cost method for verification of MNR in the Watts Bar Reservoir system.

Acknowledgements

This research was funded by National Science Foundation, Award EAR-0929154 (to EAC), the College of Arts and Sciences and the Office of Student Research (to DPG) at Appalachian State University. The magnetics laboratory at Montclair State University was supported by NSF, Award EAR/IF-0948262 to SAB. TVA provided logistical support in the field for sample collection. Neil E. Carriker, William J. Rogers and Patrick Lee kindly provided samples from the coal ash storage cell and the riverbed. Anthony Love helped to develop the magnetic separation procedure and facilitated the PLM analysis. Richard Abbott aided the XRD analysis and Edward Ficker prepared the location map.

References

- [1] Luther L. Regulating coal combustion waste disposal: issues for congress. Congr Res Sery 2010:7–5700.
- [2] Walls SJ, Jones DS, Stojak AR, Carriker NE. Ecological risk assessment for residual coal fly ash at Watts Bar Reservoir, Tennessee: site setting and problem formulation. Integr Environ Assess Manag Special Ser 2015;11:32–42. http://dx.doi.org/10.1002/jeam.1583.
- [3] Lemly AD, Skorupa JP. Wildlife and the coal waste policy debate: proposed rules for coal waste disposal ignore lessons from 45 years of wildlife poisoning. Environ Sci Technol 2012;46:8595–600.
- [4] Otter RR, Bailey FC, Fortner AM, Adams SM. Trophic status and metal bioaccumulation differences in multiple fish species exposed to coal ashassociated metals. Ecotoxicol Environ Saf 2012;85:30–6.
- [5] Scott S, Zeller C. 2D Sediment transport simulation to support the monitored natural recovery process for Watts Bar Reservoir. Abstracts: TVA-Kingston Fly Ash Release Environmental Research Symposium 2011; August 2–3, 2011. 15 p.
- [6] Carriker NE, Jones DS, Walls SJ, Stojak AR. Ecological risk assessment for residual coal fly ash at Watts Bar Reservoir, Tennessee. Integr Environ Assess Manag Special Ser 2015;11:80–7.
- [7] Tennessee Valley Authority. Kingston ash recovery project non-time-critical removal action for the river system long-term monitoring sampling and analysis plan (SAP), May 16, 2013.
- [8] Cowan EA, Seramur KC, Hageman SJ. Magnetic susceptibility measurements to detect coal fly ash from the Kingston Tennessee spill in Watts Bar Reservoir. Environ Pollut 2013;174:179–88.
- [9] Grommé C, Wright T, Peck D. Magnetic properties and oxidation of irontitanium oxide minerals in Alae and Makaopuhi Lava Lakes, Hawaii. J Geophys Res 1969;74:5277–93.
- [10] Readman PW, O'Reilly W. Magnetic properties of oxidized (cation deficient) titanomagnetite (Fe, Ti, [$]_3O_4$. J Geomag Geoelect Kyto 1972;24:69–90.
- [11] Magiera T, Jabłońska M, Strzyszcz Z, Rachwal M. Morphological and mineralogical forms of technogenic magnetic particles in industrial dusts. Atmos Environ 2011;45:4281–90.
- [12] Dunlop DJ, Özdemir Ö. Rock Magnetism: Fundamentals and Frontiers. Cambridge: Cambridge University Press; 1997.
- [13] Day R, Fuller M, Schmidt V. Hysteresis properties of titanomagnetites: grainsize and compositional dependence. Phys Earth Planet Inter 1977;13:260–7.
- [14] Banerjee SK, King J, Marvin J. A rapid method for magnetic granulometry with applications to environmental studies. Geophys Res Lett 1981;8:333–6.
- [15] King J, Banerjee SK, Marvin J, Özdmir Ö. A comparison of different magnetic methods for determining the relative grain size of magnetite in natural materials: some results from lake sediments. Earth Planet Sci Lett 1982;59:404–19.
- [16] Kutchko BG, Kim AG. Fly ash characterization by SEM-EDS. Fuel 2006;85:2537-44.
- [17] Lu SG, Chen YY, Shan HD, Bai SQ. Mineralogy and heavy metal leachability of magnetic fractions separated from some Chinese coal fly ashes. J Hazard Mater 2009;169:246–55.
- [18] Sokol EV, Kalugin VM, Nigmatulina EN, Volkova NI, Frenkel AE, Maksimova NV. Ferrospheres from coal fly ashes from Chelyabinsk coals: chemical composition, morphology and formation conditions. Fuel 2002;81:867–76.
- [19] Wang XS. Mineralogical and chemical composition of magnetic fly ash fraction. Environ Earth Sci 2014;71:1673–81.
- [20] Yang J, Zhao Y, Zyryanov V, Zhang J, Zheng C. Physical-chemical characteristics and elements enrichment of magnetospheres from coal fly ashes. Fuel 2014:135:15–26.
- [21] Zyryanov VV, Petrov SA, Matvienko AA. Characterization of spinel and magnetospheres of coal fly ashes collected in power plants in the former USSR. Fuel 2011;90:486–92.
- [22] Veneva L, Hoffman V, Jordanova D, Jordanova N, Fehr Th. Rock magnetic, mineralogical and microstructural characterization of fly ashes from Bulgarian power plants and the nearby anthropogenic soils. Phys Chem Earth 2004;29:1011–23.
- [23] Li F, Li G, Ji J. Increasing magnetic susceptibility of the suspended particles in Yangtze River and possible contribution of fly ash. Catena 2011;87:141–6.